Ecological Indicators 135 (2022) 108549

Contents lists available at ScienceDirect

Ecological Indicators

journal homepage: www.elsevier.com/locate/ecolind

Original Articles

Remote sensing-based structural and functional assessments of *Phragmites australis* diebacks in the Mississippi River Delta

Glenn M. Suir *, Christina L. Saltus, Molly K. Reif

U.S. Army Engineer Research and Development Center, Environmental Laboratory, Wetlands and Environmental Technologies Research Facility, 3909 Halls Ferry Road, Vicksburg, MS 39180-6199, USA

ARTICLE INFO

Keywords:
Remote sensing
Phragmites australis dieback
Landscape ecology
Hot spot analysis
Floristic quality index
Landscape pattern analysis

ABSTRACT

The Lower Mississippi River Delta (MRD) is dominated by *Phragmites australis* which provides a stabilizing force, protecting marsh communities from erosion and storm-related impacts. The MRD has experienced recent die-offs of *Phragmites* stands, which have coincided with a number of abiotic (hurricane and water-level) and biotic (*Phragmites* scale) stressors. During this event, previously healthy stands have died or experienced stunted growth, resulting in conversion to replacement species or to open water. This study utilized remote sensing methods to (1) evaluate changes in *Phragmites* health and distribution in the MRD through time; (2) assess changes in plant cover and floristic quality before, during, and after the dieback event; (3) evaluate changes in landscape patterns (i.e., percentage of landscape, patch density, total edge, and aggregation index); and (4) evaluate changes in channel length and width as a function of the dieback event. Normalized Difference Vegetation Index data showed an active delta landscape with below typical plant biomass/health in periods of hurricane and dieback impacts, with recovery to health values more typical for the MRD after the dieback event. Vegetation species level assessments showed the MRD landscape experienced decreasing coverage and floristic quality during the disturbance periods, and low and nominally increasing vegetation cover and quality through the dieback and recovery periods. Landscape metrics showed similar trends, where wetland areas that experienced event-related stress during the hurricane and dieback periods, showed some level of rebound during the recovery period. And finally, bank-line change analyses showed a significant increase in the rate of shortening and widening of the Mississippi River Passes since the die-back event began. This study serves as a methodological basis for deriving vegetation trend assessments and integrating those results with landscape metrics to prioritize areas of interest; all of which are essential for effective management and mitigation of aquatic nuisance vegetation.

1. Introduction

The Mississippi River Delta (MRD) is a vast natural asset that contributes goods and ecosystem services ranging from hurricane and flood protection, water quality and supply, to recreation and fisheries (Batker et al., 2010). This area, which developed through the river-dominated delta progradation phase for approximately 1000 years, has recently shifted to a destructional phase-dominated by marine processes and subsidence (Coleman et al., 1998). Through this, the delta has experienced extensive wetland loss (Couvillion et al., 2011; Suir et al., 2014), in large part, due to a complex interaction of processes and abiotic and biotic stressors, including flood control measures and altered wetland hydrology, saltwater intrusion, herbivory, reduced river sediment load, and climate events (hurricanes and sea-level rise) (White, 1993; Day et al., 2000). These conditions have made the area vulnerable to the invasion and expansion of *Phragmites australis* (common reed), which now accounts for approximately two-thirds of the low-relief exterior marshes of the MRD (Hauber et al., 2011). Since their establishment, monotypic stands of *Phragmites* have played a major role in stabilizing the outer reaches of the MRD, buffering and protecting the more diverse and susceptible interior marsh communities (Coleman et al., 1998; Hauber et al., 2011), and providing overall stability to the Delta's function, infrastructure, goods, and services.

A dieback and thinning of *Phragmites* stands in portions of the MRD was first observed in the Fall of 2016 (Knight et al., 2020). This dieback syndrome coincided with multiple stressors, including high water, high

* Corresponding author.
E-mail address: Glenn.M.Suir@usace.army.mil (G.M. Suir).

https://doi.org/10.1016/j.ecolind.2022.108549
Received 12 October 2021; Received in revised form 4 January 2022; Accepted 5 January 2022
Available online 15 January 2022

nutrient concentrations, and the infestation of *Nipponaclerda biwakoensis* (*Phragmites* scale) (Cronin et al., 2020). The *Phragmites* scale, an exotic insect native to Asia (McConnell, 1954), was first observed on *Phragmites* plants in the MRD in 2016. Marsh dieback syndrome is not uncommon in wetlands of the United States. In fact, recent diebacks have been observed in Florida, Massachusetts, South Carolina, Texas, and other parts of coastal Louisiana (Lindstedt et al., 2006; Alber et al., 2008). However, when diebacks occur in a monotypic or nearly-monotypic wetland, especially one that is in a destructional phase and susceptible to many presses and pulses, there is concern for loss of habitat structure, increasing erosion, and long-term decreasing of ecosystem stability (Duke et al., 2005). This has long been a concern for freeze-sensitive *Avicennia germinans* (black mangroves), which are currently in a 30-year expansion at their northern range limit in coastal Louisiana (Osland et al., 2020). Rapid decline of monotypic plants and recolonization by other plant species has unclear, yet potentially negative, implications for surrounding ecosystem integrity, navigation, and flood protection. Other potential negative effects could include increased flooding, erosion, and storm-related damage. One immediate concern of extensive *Phragmites* dieback is the potential for rapid soil exposure. Soil exposure could accelerate substrate degradation and erosion, resulting in reduced ecosystem productivity, and increased flood risks.

In addition to these wetland structural and functional changes, it is theorized if the stabilizing *Phragmites* stands continue to die back, the land and banks at the terminal end of Mississippi River passes will erode, shortening the length of the channels, which in turn will result in changing channel geometry—primarily bank erosion and pass widening (Sarkar, 2004). Channel morphology involves lateral erosion, channel widening, channel shortening or lengthening which are typically controlled by flow hydraulics (velocity, discharge, roughness and shear), channel configuration, load, and bed and bank material (Sarkar, 2004). Riverbank erosion in the Mississippi River system is of great concern since bank/levee failure can result in substantial flooding of lands and communities. In the MRD, bankline erosion can impact the stability of the Delta and the navigability of the River, which services the largest (based on tonnage) port district in the United States (American Association of Port Authorities, 2018). There are five federal navigation channels and four ports in the MRD (Suir et al., 2018). Southwest Pass, for example, is a primary shipping channel in the United States and could face increased wave action if the *Phragmites* marsh lining the channel should collapse (Suir et al., 2018).

With the recent dieback event comes a need to evaluate changes in *Phragmites* communities and how those changes impact structure and function within the Delta. Traditionally, field assessments have been used to evaluate wetlands, however, in situ measurements of wetland condition, function, and sustainability across large geographic areas can be impractical. However, remote sensing-based wetland evaluations provide biological metrics and indices that can be used to measure or estimate wetland condition, resilience, and recovery over time and space (Karr and Chu, 1997; Suir et al., 2020). Remote sensing data and techniques provide practical and efficient tools for evaluating wetland landscapes at a multitude of spatial and temporal scales (Broussard et al., 2018; Suir et al., 2011; Suir and Sasser, 2019). Recent advancements in remote platforms, sensors, and data processing provide novel metrics and tools for assessing and monitoring changes in vegetation community and landscape pattern, and, by extension, the impacts from and effects on system drivers and underlying ecological processes, respectively (Kupfer, 2012).

However, even with remote sensing, no single data set or analytical method can sufficiently assess the impacts of stressors in coastal wetland systems. Therefore, the goal of this study was to use a multiple-lines-of-evidence approach to evaluate *Phragmites* dieback impacts on structure and function changes in the MRD. More specifically, the objectives were to use moderate- and high-spatial resolution satellite imagery and remote sensing techniques to (1) perform a hot spot analysis to quantify changes and trends in *Phragmites* health and distribution in the MRD through time; (2) assess changes in MRD plant cover and floristic quality before, during, and after the dieback event; (3) develop *Phragmites* classification data to evaluate changes in landscape patterns (i.e., percentage of landscape, patch density, total edge, and aggregation index); and (4) evaluate changes in channel length and width as a function of the dieback event. The development and advancement of these techniques provide means for rapid tracking of extent and impacts of vegetation changes, which will ultimately provide decision support information to enhance pest and resource management.

2. Methods

2.1. Study site

The study area consists of the MRD, also known as the Bird's Foot or Plaquemines-Balize Delta, and four primary areas of interest (AOIs): Main Pass, Pass a Loutre, South Pass, and Southwest Pass (Fig. 1). The MRD is an active delta system that is located south-southeast of New Orleans, Louisiana, at the confluence of the Mississippi River and the Gulf of Mexico. The MRD area was used for moderate resolution assessments and the four AOIs were used primarily for higher-resolution assessments.

2.2. Normalized difference vegetation index and hot spot analysis

A vegetation index was used to assess the spatial and temporal changes in MRD plants in relation to the *Phragmites* dieback event. NDVI has well established correlations to photosynthetic activity, aboveground biomass, and leaf area index; and is therefore an established measure of vegetation and wetland condition (Suir et al., 2020). NDVI assessments were performed using the Landsat Thematic Mapper (TM), Enhanced Thematic Mapper (ETM), and Operational Land Imager (OLI) spaceborne sensors, which provide moderate spatial (resampled to 28 m) and temporal (16 day return) resolution imagery. The Landsat imagery, covering the period from 2010 to 2019, were acquired using the Google Earth Engine (GEE) image service. The GEE provides Tier 1 surface reflectance imagery, those meeting geometric, radiometric, and atmospheric quality requirements (Kalnay et al., 1996; Chander et al., 2009; Schmidt et al., 2013). The NDVI data were created using the standard equation (Rouse *et al.,* 1974):

$$\mathrm{NDVI} = \frac{NIR - Red}{NIR + Red} \tag{1}$$

which uses a ratio between near infrared (NIR) and red bands to measure an ecosystem's ability to capture solar energy and convert it to organic carbon or biomass (An et al., 2013).

The NDVI values range from −1 to 1, where values between −1 and zero (0) are typical of non-vegetation features (i.e., water, cloud, and impervious surfaces), and those between 0.2 and 1.0 are typical of green, healthy vegetation (Datt, 1999; Sims and Gamon, 2002). Generally, the higher the NDVI value, the higher the biomass, productivity, and vigor of the vegetation. All non-marsh features within the study area were excluded from each image by removing NDVI values less than zero (<0) (Reif et al., 2011). In an effort to reduce seasonal variations, this study focused the NDVI calculations using imagery collected during the latter half of the *Phragmites* growing season (August to October) (Howard and Turluck, 2013). The MRD and individual AOIs were used to calculate mean NDVI values for each AOI.

Remote sensing- and field-based metrics were used to identify and further assess trends within periods prior to, during, and after the *Phragmites* dieback event. The end-of-growing season Landsat-derived NDVI data were used to evaluate spatial and temporal changes in plant health. The analysis was performed using a sequence of linear regression analysis and a Getis-Ord Gi* hot spot function. The linear regression analyses were performed using the Curve Fit v10.1 (De Jager

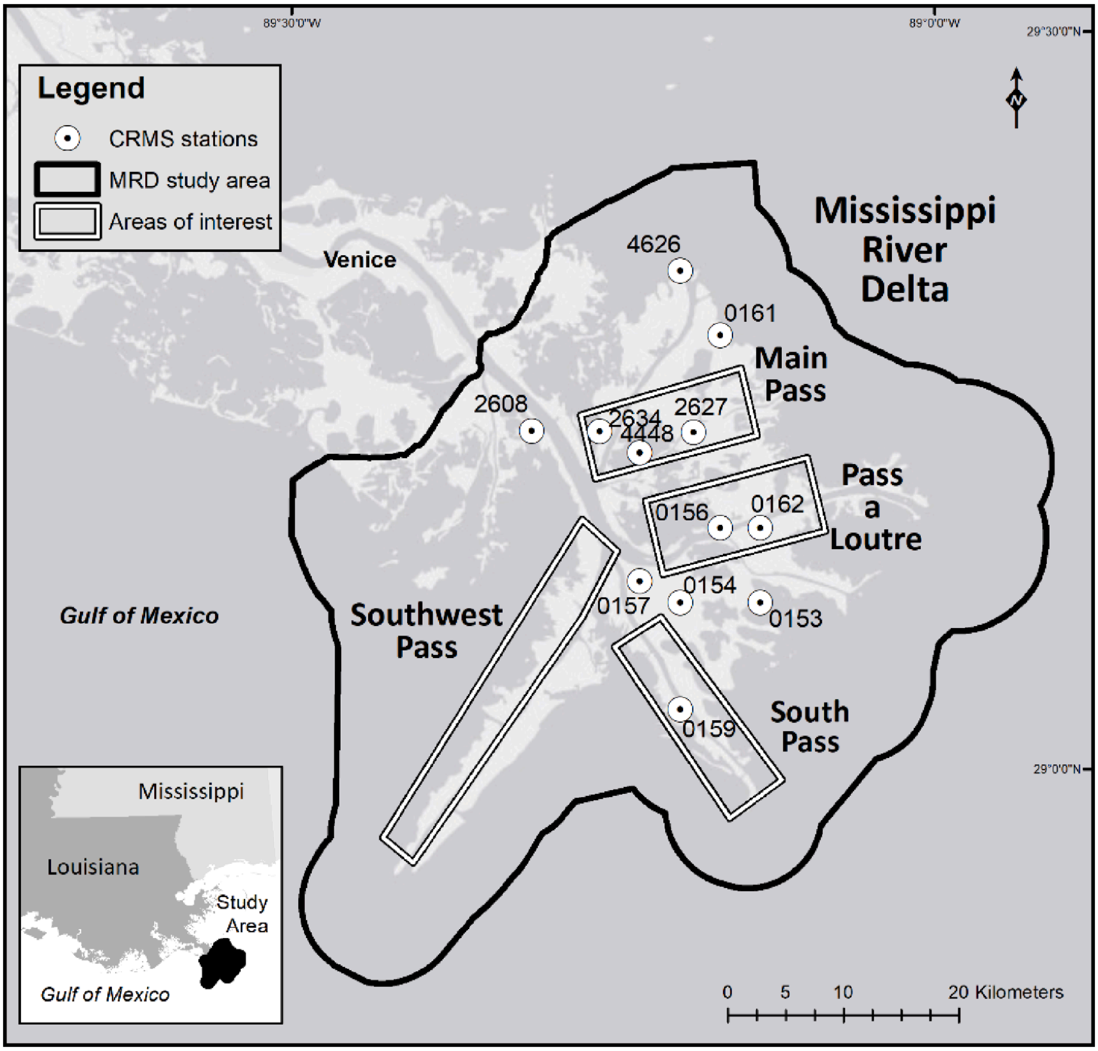

Fig. 1. Location map of the Mississippi River Delta, Southwest Pass, Main Pass, Pass a Loutre, and South Pass study areas.

and Fox, 2013) ArcGIS Desktop 10.7.1 (Environmental Systems Research Institute (ESRI) 2012) extension to conduct linear regression analyses within each period (i.e., before, during, after dieback; and across the entire period of record). The Curve Fit extension, which uses the range of NDVI values at each pixel location (regressed over time), was used to generate raster surfaces of regression model parameter estimates, standard errors, and goodness-of-fit (De Jager and Fox, 2013).

The Getis-Ord Gi* tool in ArcGIS Pro Release 2.5.2 (ESRI, 2020) was used to evaluate NDVI hot spot areas within the MRD (Choudhary et al., 2015). The Curve Fit generated raster-based linear regression parameter estimates were converted to point data and processed using the False Discovery Rate (FDR) correction and Inverse Distance weighting within the Getis-Ord Gi* tool. The Getis-Ord Gi* statistics and standardized Z scores are based on expected values E (Gi*) and the variances (VAR (Gi*)), which are mathematically expressed by the equation:

$$G_i^*(\mathrm{d}) = \frac{\sum_{j=1}^{n} w_{ij}(d)x_j}{\sum_{j=1}^{n} x_j} \quad (2)$$

where, d is the distance threshold, w_{ij} is the weight of target neighbor pair, and x_j is the severity index at location j (Choudhary et al., 2015). The results of the Getis-Ord Gi* analyses identify statistically significant high value areas, or those that are also surrounded by high valued neighbors.

2.3. Vegetation cover and floristic quality index

This study also used vegetation survey data from twelve existing Coastwide Reference Monitoring System (CRMS) stations (Fig. 1). CRMS is a network of approximately 390 monitoring sites in coastal Louisiana designed to collect, process, and analyze physical, chemical, biological, and geospatial data to characterize coastal wetland landscapes inside and outside of restoration project sites (Cretini et al., 2011). Vegetation cover and floristic quality changes within the MRD were performed using CRMS station data. Within the CRMS program, emergent vegetation are typically surveyed annually during the period of peak biomass (Folse et al., 2014), however some gaps in collection can occur due to site access or other limitations. The CRMS Data Download service was used to acquire all existing vegetation data from the twelve CRMS stations within the MRD (Fig. 1) during the CRMS period of record (2006 to 2019; CPRA, 2019). These vegetation data consist of species identification, percent cover (Braun-Blanquet scale), and floristic quality index (FQI, described below). The identification and percent cover data were used to assess change in *Phragmites* cover and shifts to other plant species during the 2010 to 2019 period of analysis.

The FQI is a weighted metric that assesses the condition of plant communities using estimates of vegetation quantity and quality. The FQI is based on a measure of vulnerability, called the Coefficient of Conservatism (CC), together with the richness of a plant community (Gianopulos, 2014). CC values range from zero (not conservative) to ten (conservative and highly ecologically sensitive) and are assigned to individual plant species within a local flora by a panel of experienced botanists (Little, 2013; Bourdaghs et al., 2006). CC classes include invasive plant species (CC value of 0), disturbance species (CC = 1–3), vigorous wetland communities (CC = 4–6), common species (CC = 7–8), and dominant wetland species (CC = 9–10). Details and methods of the FQI system used in this study are described in Suir and Sasser (2017). FQI scores, ranging from 0 to 100, provide estimates of vegetation condition and maturity. Low FQI values can be indicative of early successional vegetation communities, highly disturbed or early post-disturbance evolution, or conditions that negatively impact natural or managed wetlands. Conversely, high FQI values are more typical in mature, stable, and un-disturbed wetlands.

2.4. Landscape metrics

Landscape metrics were used to evaluate changes in extent and configuration of the MRD *Phragmites* communities before, during, and after the recent dieback event. The FRAGSTATS landscape pattern analysis software (version 4.2.1; McGarigal et al., 2012) was used to compute landscape metrics using *Phragmites* classification data generated from high-resolution MAXAR (i.e., GeoEYE, Quickbird, and WorldView) imagery. Images from the MAXAR constellation of satellites provide high spatial (1.24 to 2.62 m multispectral) and temporal (1–3 day sensor returns) resolution data that are useful for estimating short-term landscape variation linked to disturbance events and/or prevailing environmental conditions (Suir et al., 2020). Cloud-free MAXAR satellite imagery collected in 2013, 2016, and 2020 were acquired using the Enhanced Viewer Web Hosting Service. The images were geometrically and atmospherically corrected and transformed to reflectance using the QUick Atmospheric Correction (QUAC) algorithm in ENVI 5.5 software (ITT, 2009; Mutanga et al., 2012).

A supervised classification routine was used to classify imagery into two target classes, *Phragmites* and non-*Phragmites*. The *Phragmites* classification used the Maximum Likelihood Classifier (MLC) in ENVI 5.5 and ground verification data from multiple sources: CRMS sites, field observations (field surveys performed by Louisiana State University researchers in Fall of 2018), and additional "heads-up" digitizing methods (i.e., drone thruthing and user-based identifications; Suir et al., 2021). The ground verification data are a critical component of wetland classification because they are necessary for training supervised classification algorithms, validating classified areas, and performing error evaluations (Jensen, 2015). Seventy percent of the ground verification data were used to train the classification algorithm, while thirty percent were set aside to assess the accuracy of the classification results. Within the trained MLC system, each pixel was assigned to the class with the highest probability and all pixels in the image were labelled as either *Phragmites* or non-*Phragmites* (Carle, 2013). Lastly, a quantitative classification accuracy was performed using validation sites and traditional error matrix methods (Jollineau and Howarth, 2008).

The landscape metrics selected for use in this study include class area (km^2), percent land, patch density, total edge (km), and aggregation index. This study utilized the *Phragmites* classified data to quantify area and pattern metrics during select periods (i.e., before, during, and after dieback event). The class area (CA), which equals the sum of the areas (m^2) of all patches of the corresponding patch type, divided by 1,000,000 (to convert to square kilometers (km^2), is quantified using the equation:

$$CA = \sum_{j=1}^{n} a_{ij}\left(\frac{1}{1,000,000}\right), \quad (3)$$

where a_{ij} *is the area of patch ij*. The percentage of land (PLAND) is the proportional abundance of land within the landscape and is quantified using the equation:

$$PLAND = P_i = \frac{\sum_{j=1}^{n} a_{ij}}{A}(100), \quad (4)$$

where P_i is the proportion of the landscape occupied by patch type (class) *i*, a_{ij} is the area (m^2) of patch *ij*, and *A* is the total landscape area (m^2). Patch density (PD) provides a general measure of wetland or plant community fragmentation, and is quantified using the equation:

$$PD = \frac{n_i}{A}(10,000)(100), \quad (5)$$

where, n_i is the number of patches in the landscape of patch type *i*, and *A* is the total landscape area (m^2). Total edge (TE) is the sum of the lengths (m) of all edge segments in the landscape, and is quantified using the equation:

$$TE = E, \quad (6)$$

where E is the total length (m) of class edge in the landscape. Aggregation index (AI) provides a measure of landscape condition that positively correlate to wetland or plant species integrity and stability (Suir et al., 2013; Couvillion et al., 2016). AI has evolved as a primary metric for linking structure to ecosystem function and is defined as the frequency with which different pairs of patch types appear side-by-side in a landscape (McGarigal, 2015). This index, which was used to assess *Phragmites* configuration changes over time, is quantified using the class-level equation:

$$AI = \left[\sum_{i=1}^{n}\left(\frac{g_{i,i}}{\max\_g_{i,i}}\right)\right](100), \quad (7)$$

where $g_{i,i}$ is the number of like adjacencies between pixels of patch type *i* (class), $\max\_g_{i,i}$ is the maximum number of like adjacencies between pixels of patch type *i* (class) (He et al., 2000; McGarigal, 2015). Together, these class-level metrics were used to evaluate spatial and temporal changes and trends in *Phragmites* stands as a function of the recent dieback event in the MRD.

2.5. Channel morphology

Two assessments were conducted to evaluate changes in bankline position (channel width) and length (channel length). The bankline position and length assessments used existing Mississippi River hydrographic survey data as well as high resolution imagery from which bankline positions were delineated (Table 1). The existing Mississippi River surveys consist of a series of hydrographic data (data available in raster and vector format for older and newer surveys, respectively) from 1949 through 2004, and were supplemented with bankline delineations developed using high spatial resolution air- and space-borne imagery from 1998, 2010, 2013, and 2019 (Table 1).

Changes in channel width were calculated for each year/period of bankline data using bankline positions and transects at 1 km intervals from the head-of-passes to the terminal end of each pass (Fig. 2) (Chaiwongsaen and Choowong, 2019). The length of each pass was also calculated by determining the mid-channel length from the upper-most river transect for each pass to the terminal end of the left and right bank (Fig. 2). Left and right banks are defined with reference to an observer facing downstream (Kaufmann, 2000). The length of each pass was calculated as the mean length of the left and right bank for each year/period of bankline data.

3. Results and discussion

3.1. Plant biomass and hot spot assessments

Fig. 3 shows mean NDVI values and the trajectories of values in each AOI through time. These represent all end of growing season conditions.

Table 1
Specifications of hydrographic surveys (aerial photos) and air- and space-borne imagery used to delineate banklines in the Mississippi River Delta.

Data type	Satellite-sensor	Date (year)	Resolution (m) or scale	Coverage (passes)	Source
Hydrographic survey	Aerial photos	1949–1952	1: 20,000	Loutre, South, Southwest	USACE
Hydrographic survey	Aerial photos	1961–1963	1: 20,000	Loutre, South, Southwest	USACE
Hydrographic survey	Aerial photos	1973–1975	1: 20,000	Loutre, South, Southwest	USACE
Hydrographic survey	Aerial photos	1991–1992	1: 12,000	Loutre, South, Southwest	USACE
Bankline delineations	DOQQ	1998	1: 10,000	Main, Loutre, South, Southwest	USGS
Hydrographic survey	Aerial photos	2004	1: 20,000	Main, Loutre, South, Southwest	USACE
Bankline delineations	QuickBird	2010	2.6	Main, Loutre, South, Southwest	MAXAR
Bankline delineations	WorldView-3	2013	1.24	Main, Loutre, South, Southwest	MAXAR
Bankline delineations	GeoEYE	2019	1.84	Main, Loutre, South, Southwest	MAXAR

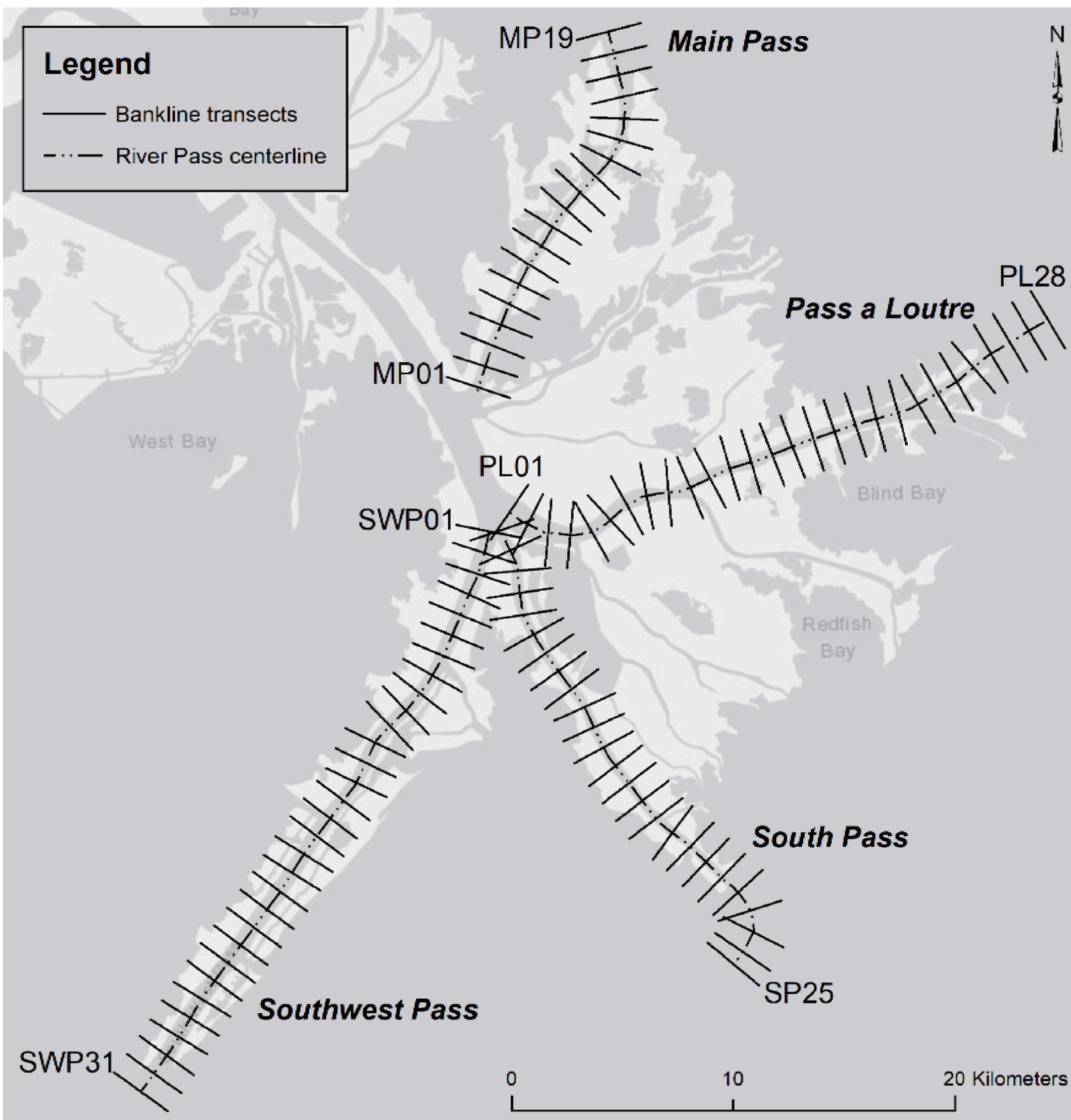

Fig. 2. Centerlines and transects for Main Pass, Pass a Loutre, South Pass, and Southwest Pass.

The four AOIs largely correspond to the changes in NDVI values across the entire MRD, with Main Pass and Southwest Pass being the maximum and minimum values, respectively, for most dates. The full period of analysis (2010 to 2019) can be separated into three distinct periods. The period from 2010 to 2013 (hurricane period) where the mean NDVI values were relatively low and exhibited fluctuations due to considerable climate events (i.e., Tropical Storm Ida (2009) and Hurricane Isaac (2012)), the period from 2013 to 2016 (dieback period) where NDVI values were lowest due to biotic and abiotic factors, and the 2016 to 2019 period (recovery period) where the mean NDVI values increased substantially (recovery period after the principal dieback event). The hurricane period (2010 to 2013) experienced an overall low but increasing plant biomass/health vegetation recovered after storms Ida and Isaac (vegetative recovery typically occurs by the end of the next full growing season after a disturbance event; Carle et al., 2015; Steyer et al., 2013), the dieback period (2013 to 2016) experienced low and

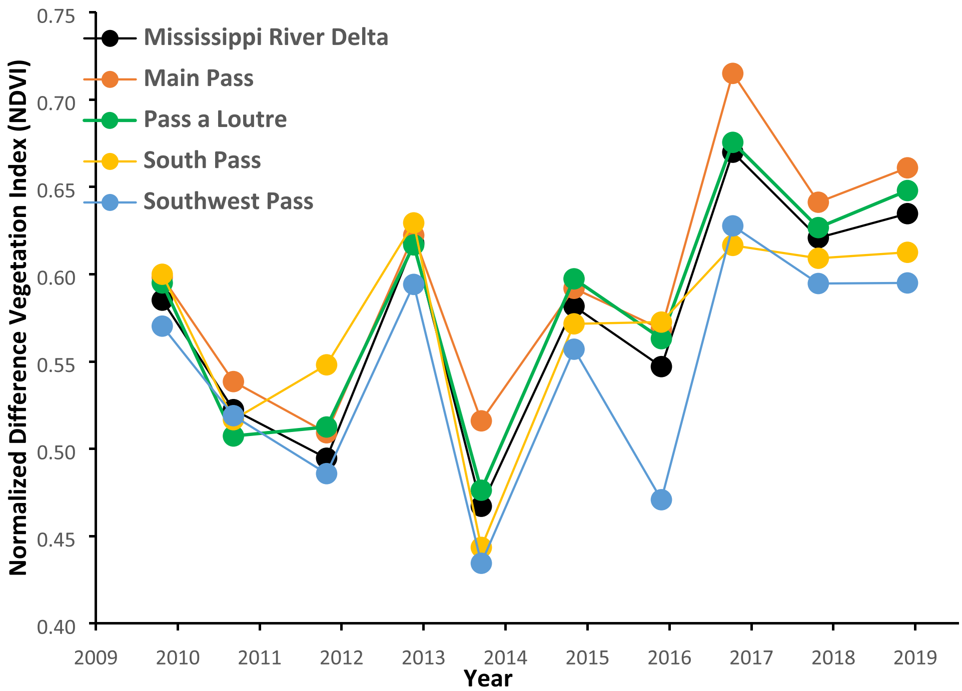

Fig. 3. Landsat-derived mean NDVI trajectories from 2010 to 2019 (within growing season) for the Mississippi River Delta, Main Pass, Pass a Loutre, South Pass, and Southwest Pass assessment units.

decreasing plant biomass/health, and the recovery period (2016 to 2019) experienced high and increasing plant biomass/health as plants recovered after the dieback event.

Although Fig. 3 provides a general assessment of temporal changes in mean NDVI values across the MRD and AOIs, it lacks the detail required to assess both temporal and spatial changes in plant health. Fig. 4 contains the linear regression results which illustrates both spatial and temporal changes in NDVI (change per year per pixel) within the hurricane, dieback, and recovery periods. Within the hurricane period (2010 to 2013) vegetation experienced moderate storm-induced reductions in NDVI across the MRD. There are small regions where decreases in NDVI were more distinct (red squares in Fig. 4; northwest of the Mississippi River main channel and between Pass a Loutre and South Pass), and areas where increases were more distinct (green squares in Fig. 4; near the outflow of Main Pass and South Pass). During the dieback period (2013 to 2016) the NDVI change rates were more irregular, with higher loss and gain rates mottled throughout the MRD. The regions of highest decreasing NDVI change rates were at the down-river reaches and periphery of the MRD. Most of the areas that experienced reductions in NDVI during the dieback period experienced substantial increases in NDVI during the recovery period (2016 to 2019). Although the MRD largely experienced increasing NDVI values during the recovery period, there were some areas (downstream portions of South Pass and wetland between Main Pass and Pass a Loutre) with decreasing NDVI change rates.

Fig. 5 shows the results of the Getis-Ord Gi* hot spot analysis. The hot spot analysis creates a new output feature data layer consisting of the Gi* confidence level bins. Fig. 5 shows the hot spot (-1, -2, and -3,

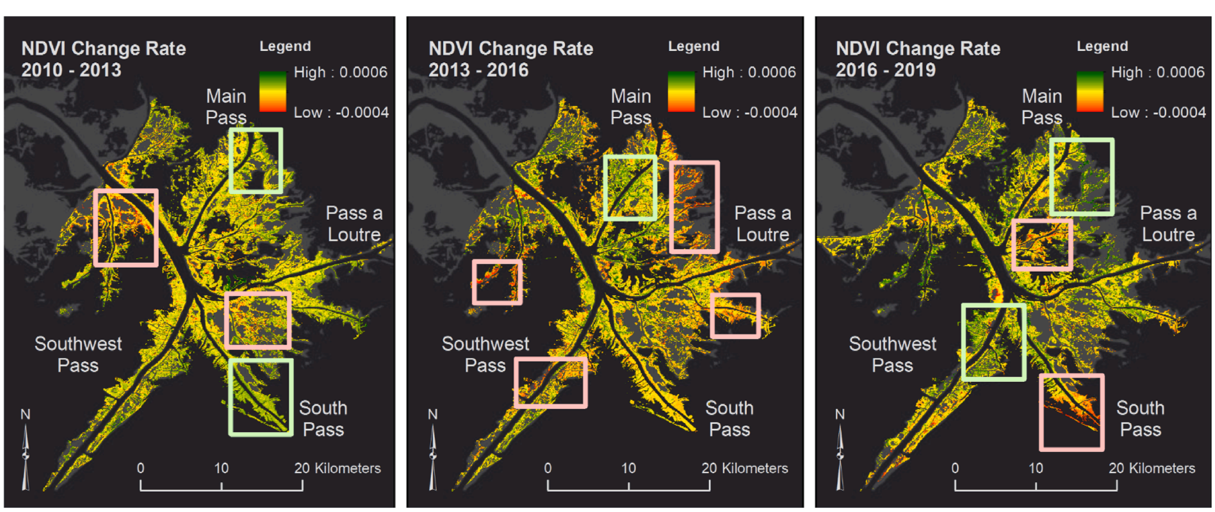

Fig. 4. Landsat-derived NDVI change rate per pixel (per year) for the hurricane period (2010–2013), *Phragmites* dieback period (2013–2016), and recovery period (2016–2019) in the Mississippi River Delta. Green squares represent distinct regions of decreasing NDVI and red squares identify regions of decreasing NDVI. (For interpretation of the references to colour in this figure legend, the reader is referred to the web version of this article.)

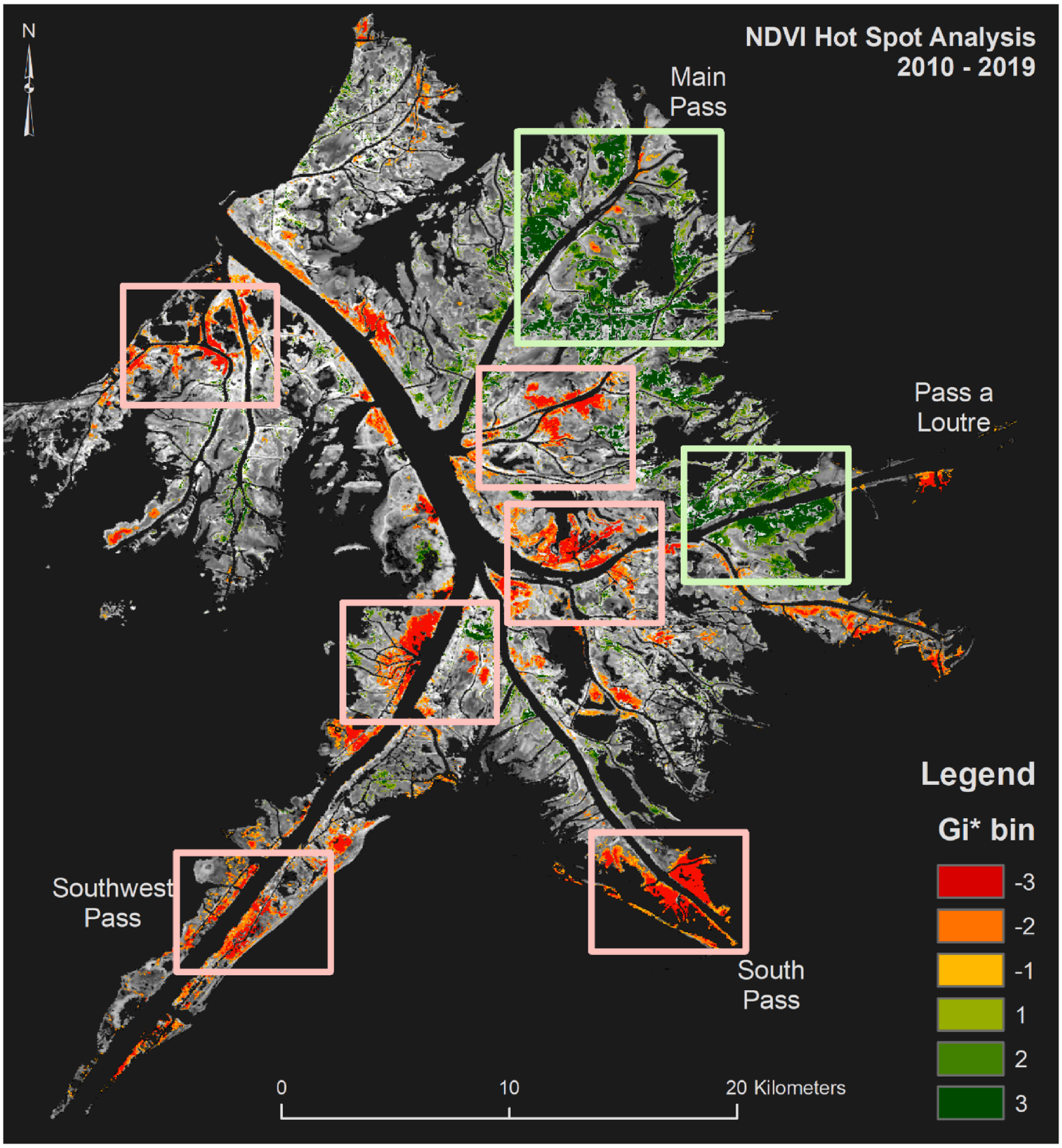

Fig. 5. Getis-Ord Gi* hot spot analysis using Landsat-derived NDVI from 2010 to 2019 for the Mississippi River Delta. Green squares represent hot spot areas with significant increases in biomass/health across the period of analysis and red squares represent areas of significant decreases. (For interpretation of the references to colour in this figure legend, the reader is referred to the web version of this article.)

which are represented by the colors yellow, orange, and red, respectively) and cold spot (1, 2, and 3, represented by light to dark greens, respectively) bins. The hot spot areas (red squares in Fig. 5), which represent regions within the MRD where vegetation biomass and health experienced significant reductions across the entire period of analysis (2010 to 2019), are found in the western part of the wetlands between Main Pass and Pass a Loutre, along Southwest Pass, and at the southern extent of South Pass wetlands. The cold spot areas (green squares in Fig. 5), which represent regions where vegetation biomass and health experienced significant increases across the period of analysis, are found primarily at the eastern portion of the MRD within wetlands near Main Pass and Pass a Loutre. It should be noted that the cold spot areas are those that experienced vegetative recovery after NDVI loss rates during the dieback period. While the NDVI assessments provide general measure of plant health and trends of *Phragmites*, it also includes impacts to other plants present in the MRD. This application is suitable in this situation because the Delta is comprised largely of *Phragmites*.

3.2. Changes in plant cover and floristic quality

Fig. 6 shows the total vegetation cover (%), the average vegetation cover (%) by species, and the floristic quality index, separated by CRMS site and year. There were 77 unique plant species observed across all MRD CRMS stations from 2006 to 2019. Species with cover values < 3% in a given year were categorized as “other.” The early CRMS vegetation surveys, which began in 2006, show a delta that was dominated by *Phragmites* in all of the most southern sites, and by *Colocasia esculenta*, *Polygonum glabrum*, *Sagittaria lancifolia*, *Sagittaria latifolia*, *Sagittaria platyphylla*, *Spartina alterniflora*, *Schoenoplectus deltarum*, and *Vigna luteola* in the northernmost sites (Fig. 6). For the *Phragmites* dominated sites, the cover and FQI values underwent nominal change during the hurricane period, while the sites dominated by non-*Phragmites* species experienced substantial reductions in cover and FQI values. For the sites dominated by non-*Phragmites* species, the dieback period consisted of decreased percentages of cover and reductions in FQI scores.

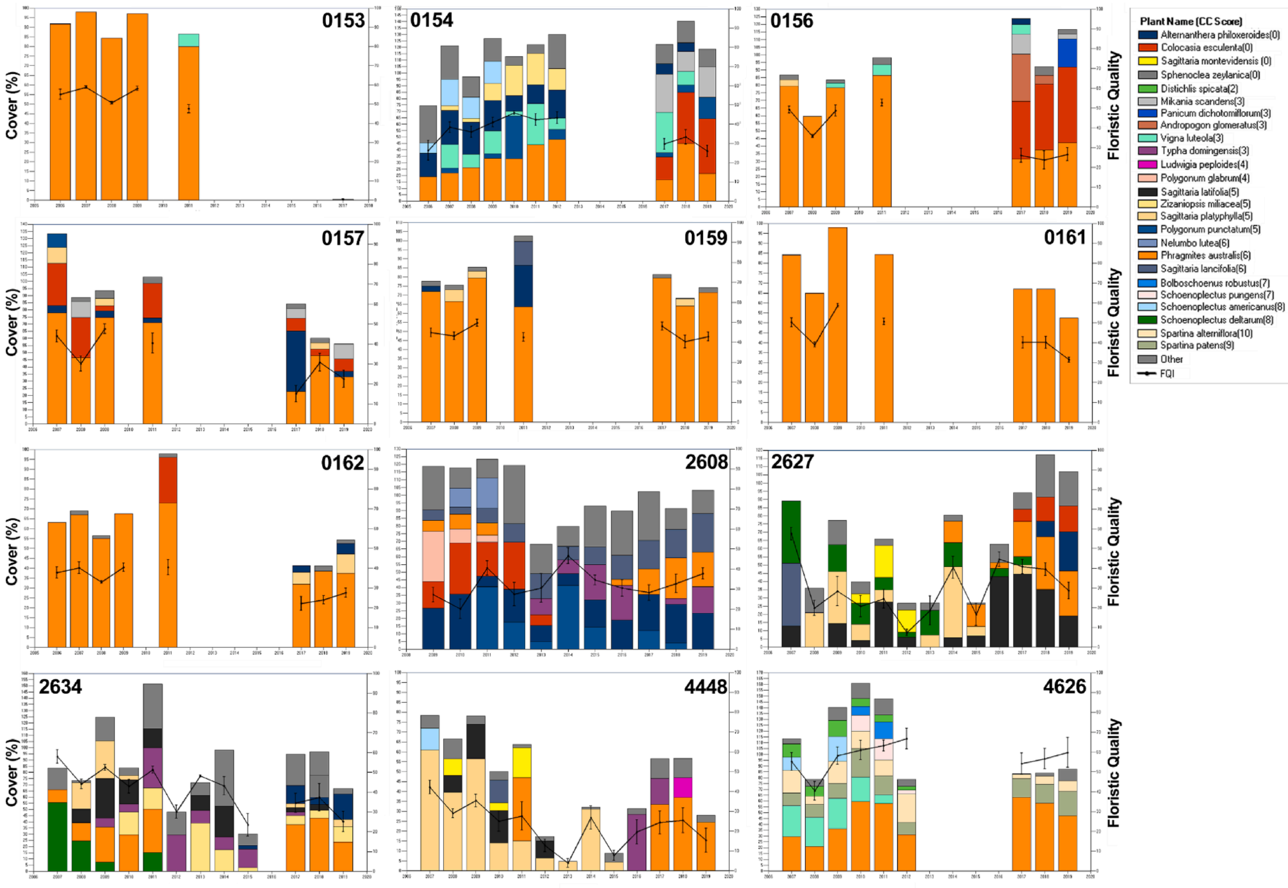

Fig. 6. Cover values (percentages) and FQI scores from the twelve CRMS stations within the MRD. Orange bars represent the percentage of *Phragmites* cover for each year within CRMS station (CPRA 2019). (For interpretation of the references to colour in this figure legend, the reader is referred to the web version of this article.)

Unfortunately, there are data gaps during the dieback period for all of the *Phragmites*-dominated sites. During the recovery period, the sites dominated by non-*Phragmites* species experienced substantial increases in *Phragmites* cover, when compared to previous periods, while sites previously dominated by *Phragmites* experienced substantial reductions in *Phragmites* cover (Fig. 6). For most CRMS sites the cover and FQI values were substantially lower during the recovery period than either the hurricane or dieback periods (exceptions are sites 2608 and 2627). The lower FQI scores are, in some cases, due to the lower cover values, while at other sites the lower scores are due, in part, to the establishment of disturbance species (i.e., *Colocasia esculenta* and *Alternanthera philoxeroides)* which often serve as indicators of stressed systems (Suir 2018). Interestingly, it is observed that species level assessments differ somewhat from the landscape-based NDVI assessments. The species level assessments show lower and decreasing FQI values during the recovery period, while the landscape-based assessments show higher and increasing NDVI values in the recovery period. This could be a function of scale, where the CRMS stations provide data at a limited number of sites within the MRD, and thus, may not represent trends in the larger geographic extent; or where the NDVI assessments include biomass/ health of all species within the MRD, and thus, may not represent species-specific trends.

Fig. 7 provides the FQI scores for all of the *Phragmites*-dominant CRMS sites (Fig. 6), by year. Fig. 7 also provides the mean *Phragmites* FQI scores by year for all sites across the CRMS period of record (2006 to 2019), but differentiated by period ("pre" period is from 2006 to 2010, hurricane period is 2010 to 2013, dieback period is 2013 to 2016, and recovery period is 2016 to 2019). The FQI scores for the *Phragmites-domintated sites* (colored lines and markers, Fig. 7) ranged from approximately 30 to 60 during the pre- and hurricane periods, and dropped to scores that ranged from approximately 1 to 48 during the dieback and recovery periods. These trends were also observed in the mean FQI scores from all CRMS sites in the MRD (solid and dashed black lines). The trends in mean FQI scores across the full period of analysis (2006 to 2019) show higher and more stable FQI scores in the pre-period, lower and decreasing scores in the hurricane period, and lower with slight increasing FQI rates in the dieback and recovery periods. In all, the FQI scores within the MRD were below the ideal range (70) for fresh and intermediate marsh in an active deltaic plain (Cretini et al., 2012). This is primarily due to reductions in vegetation cover, and the presence and establishment of plants with low CC scores. The lower CC scores are controlled by the dominant *Phragmites* plant (a rigorous wetland plant with CC score of 6), and the other persistent non-native, opportunistic species (i.e., *Colocasia esculenta* and *Alternanthera philoxeroides*) within the Delta (Plitsch, 2017).

3.3. Class-level pattern analysis

An example of the *Phragmites* classification data that were generated using the Maximum Likelihood classification is provided in Fig. 8. The *Phragmites* classification data were created using high-resolution satellite imagery from 2013, 2016, and 2020. These classifications, which were assessed using ground verification data and standard confusion matrices, had Overall Accuracies (OA) of 93.581, 94.257, and 93.919; and Kappa values of 0.871, 0.879, and 0.878; for the 2013, 2016, and 2020 classifications, respectively. These high accuracy values are possible because of the high spatial resolution of the imagery and the physical and spectral uniqueness of *Phragmites australis* in relation to

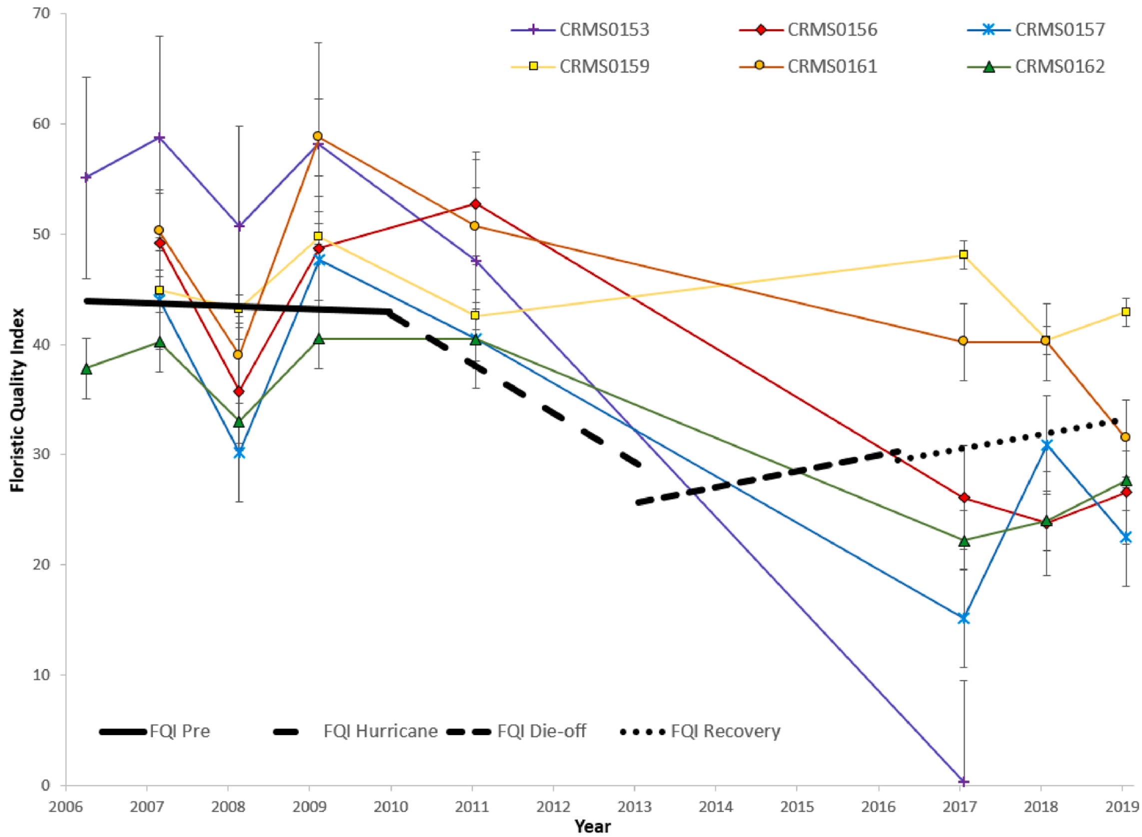

Fig. 7. FQI and cover trends at *Phragmites*-dominant CRMS station within the Mississippi River Delta between 2006 and 2019.

other vegetation types in the MRD.

Table 2 provides the class-level landscape metrics (i.e., class area, percentage of land, patch density, total edge, and aggregation index) that were computed using the *Phragmites* classification data (2013, 2016, and 2020) from within the four AOIs. Together, these metrics provide an estimate of change and recovery experienced by *Phragmites* during the hurricane, dieback, and recovery periods. For total *Phragmites* class area (CA) and the related percentage of land, the study AOIs experienced different trends. The Main Pass area experienced losses across all periods; Pass a Loutre and South Pass experienced loss of *Phragmites* from 2013 to 2016, but then experienced some *Phragmites* recovery by 2020; and Southwest Pass experienced increasing *Phragmites* area (0.2 km^2) between 2013 and 2016, followed by an additional 3.8 km^2 gain by 2020. These differences are indicative of areas that were subjected to stressors at different times. This is corroborated by the NDVI trend assessment which shows the AOIs experiencing biomass and health declines during different periods. For patch density (PD) and total edge (TE), the four AOIs all experienced similar trends. Increases in PD and TE were observed for all AOIs between 2013 and 2016, followed by relatively moderate to nominal decreases between 2016 and 2020. PD and TE changes are indicative of a wetland system that initially underwent vegetative loss, both at marginal and interior locations, but then recovered in some of those areas. Similarly, the four AOIs experienced comparable trends in aggregation index (AI). The AOIs had initial AI scores ≥98.4, but then experienced decreases and increases by 2016 and 2020, respectively. Changes in AI are also indicative of *Phragmites* landscapes that became fragmented or disaggregated during the dieback period, but then experienced some recovery of *Phragmites* during the recovery period. The class-level metrics are useful because they provide measures of landscape patterns which allow for a better understanding of how the *Phragmites* mono-culture changed spatially over time.

3.4. Changes in channel morphology

Examples of the river pass centerlines (white dashed line), transects (white dotted line), and banklines (yellow, orange, and red lines) that were used for the river length and bankline morphology assessments are provided in Fig. 9. The centerlines were used to measure the average length (mean of left and right side banklines) of each river pass. To evaluate potential impacts of the dieback event, trends in channel morphology were separated into two primary periods, the historical period (1949 to 2013) and the dieback/recovery period (2013 to 2019). Average change in length from 1949 to 2019 is shown in the inset table in Fig. 9. Pass a Loutre experienced the greatest change rate at −0.038 km/yr, and Southwest Pass experienced the lowest rate, at −0.013 km/yr. Fig. 9 also shows the river length change rate for the dieback and recovery periods, 2013 to 2019, allowing for the evaluation of loss attributed, at least in part, to the dieback event. During these periods, Pass a Loutre experienced a river length change rate of −0.099 km/yr, while Main Pass had a change rate of −0.015, which is a lower rate than what Main Pass experienced across the 1949 to 2013 period. This assessment indicates that although the River Passes have shortened since the 1940s, the rates of shortening have increased (in all but Main Pass) since the dieback event began in 2013.

Fig. 10 illustrates the bankline change rates (measured as the change in Pass width in m/yr) at each transect across Passes Main, a Loutre, South, and Southwest. Across all transects, South and Southwest Passes experienced the largest rates of bankline erosion, having only four of 56 transects experiencing Pass narrowing. The channel width change rates at Pass a Loutre transects fall primarily between South/Southwest Pass and Main Pass rates. Approximately half of the Pass a Loutre transects experienced channel narrowing between the 1940 s and 2019, while only one Main Pass transect experienced channel widening during the same period. Table 3 provides the channel width change rates for each

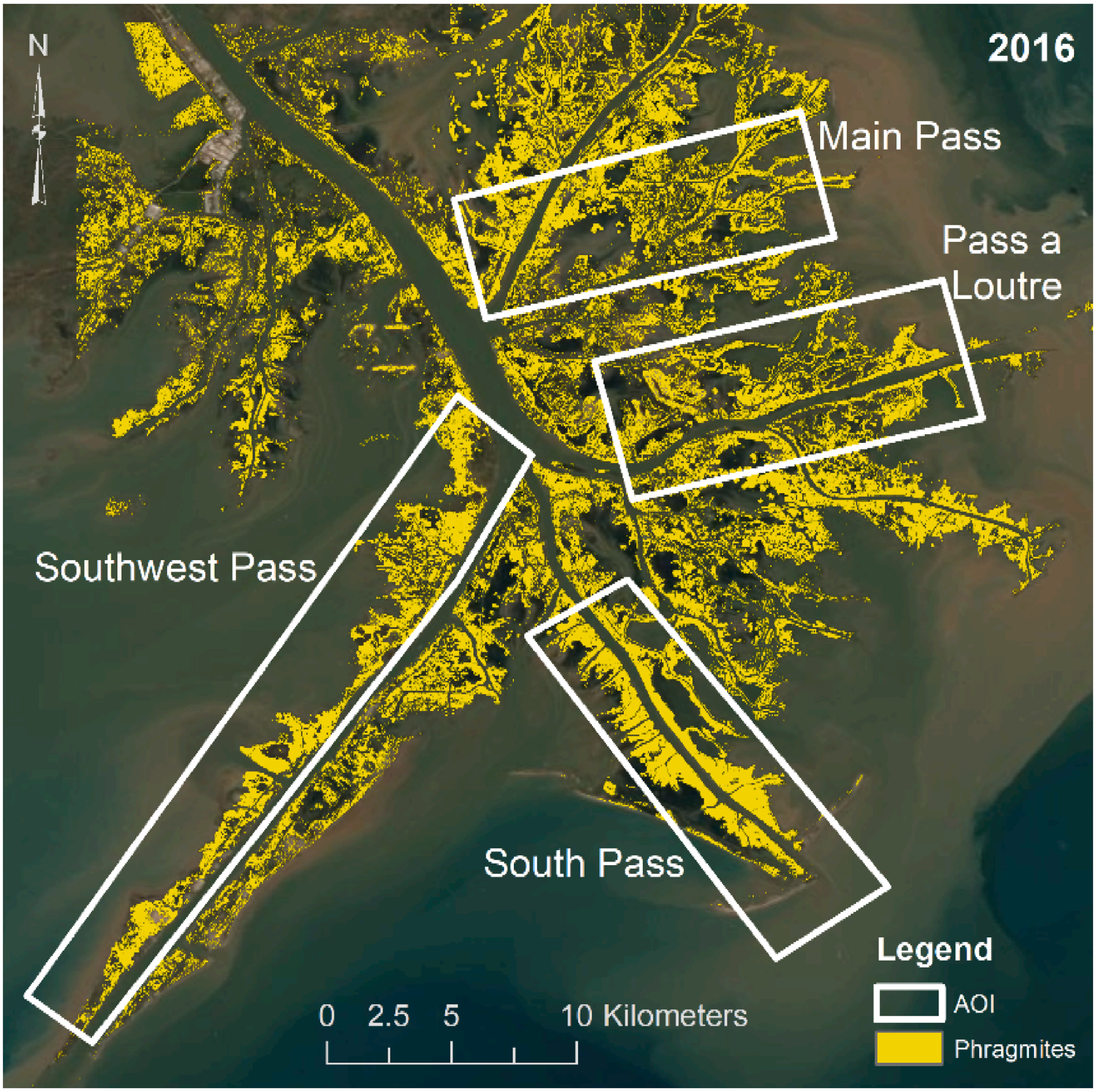

Fig. 8. *Phragmites* classification data derived from 2016 MAXAR imagery from the MRD.

Table 2
Mean values of class-level landscape metrics (class area, percent land, patch density, total edge, and aggregation index) for each of the study areas of interest.

Year	Area of interest	Type	Class area (km^2)	Percent land	Patch density	Total edge (km)	Aggregation index
2013	Main Pass	*Phragmites*	24.7	38.9	34.9	1052	98.5
2016	Main Pass	*Phragmites*	22.2	34.9	234.2	2307	96.2
2020	Main Pass	*Phragmites*	21.8	34.4	168.5	2129	96.5
2013	Pass a Loutre	*Phragmites*	25.2	35.0	35.3	1039	98.5
2016	Pass a Loutre	*Phragmites*	21.3	29.6	197.2	2223	96.3
2020	Pass a Loutre	*Phragmites*	22.1	30.8	144.8	2052	96.7
2013	South Pass	*Phragmites*	20.3	29.1	15.2	609	98.9
2016	South Pass	*Phragmites*	19.2	27.5	70.8	843	98.4
2020	South Pass	*Phragmites*	19.7	28.2	30.0	715	98.7
2013	Southwest Pass	*Phragmites*	20.7	21.0	18.8	937	98.4
2016	Southwest Pass	*Phragmites*	20.9	21.2	73.5	1434	97.5
2020	Southwest Pass	*Phragmites*	24.7	25.0	52.3	1409	98.0

AOI during the period of record prior to the recent dieback event (1949 to 2013) and the dieback/recovery periods (2013 to 2019). The historical change rates ranged from −3.20 to 2.49 m/yr for Main Pass and South Pass, respectively. The change rates during the dieback and recovery periods ranged from −1.70 to 5.72 m/yr for Main Pass and Southwest Pass, respectively. Main Pass experienced channel narrowing across all periods, but had higher rates of narrowing during the 1949 to 2013 period. Some significant changes in channel width were observed

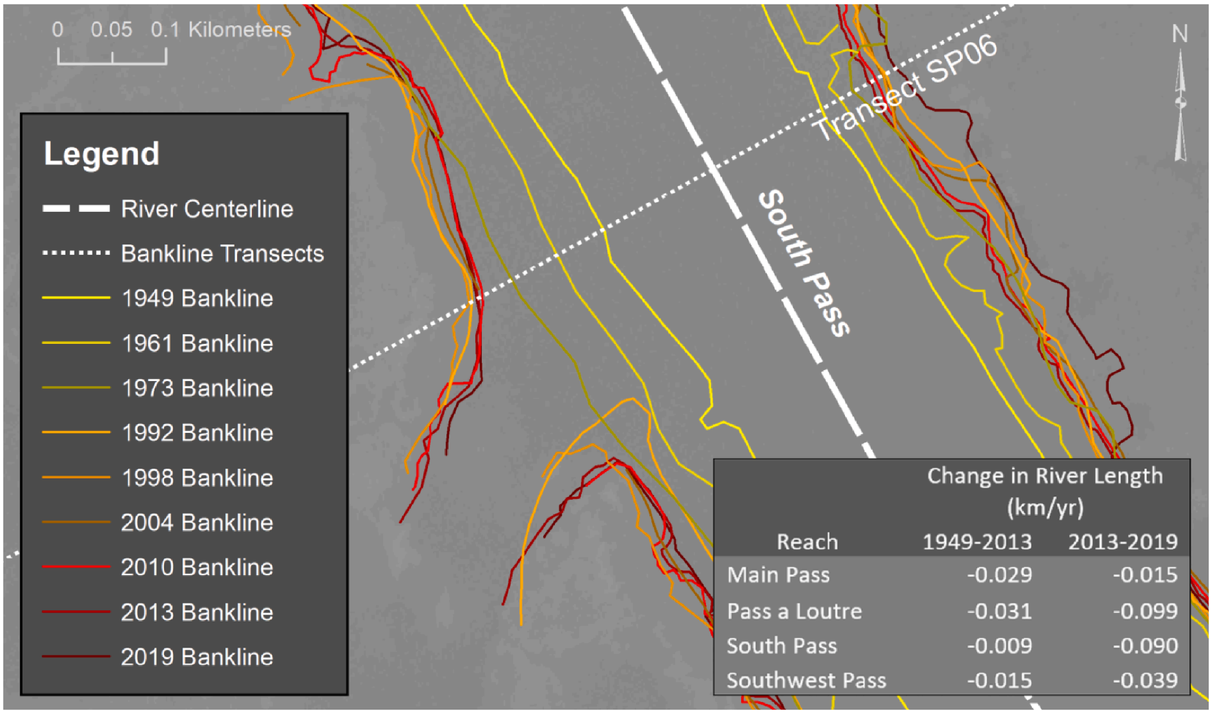

Fig. 9. Example of bankline position (South Pass) and length change (all Passes; inset) from 1949 to 2019.

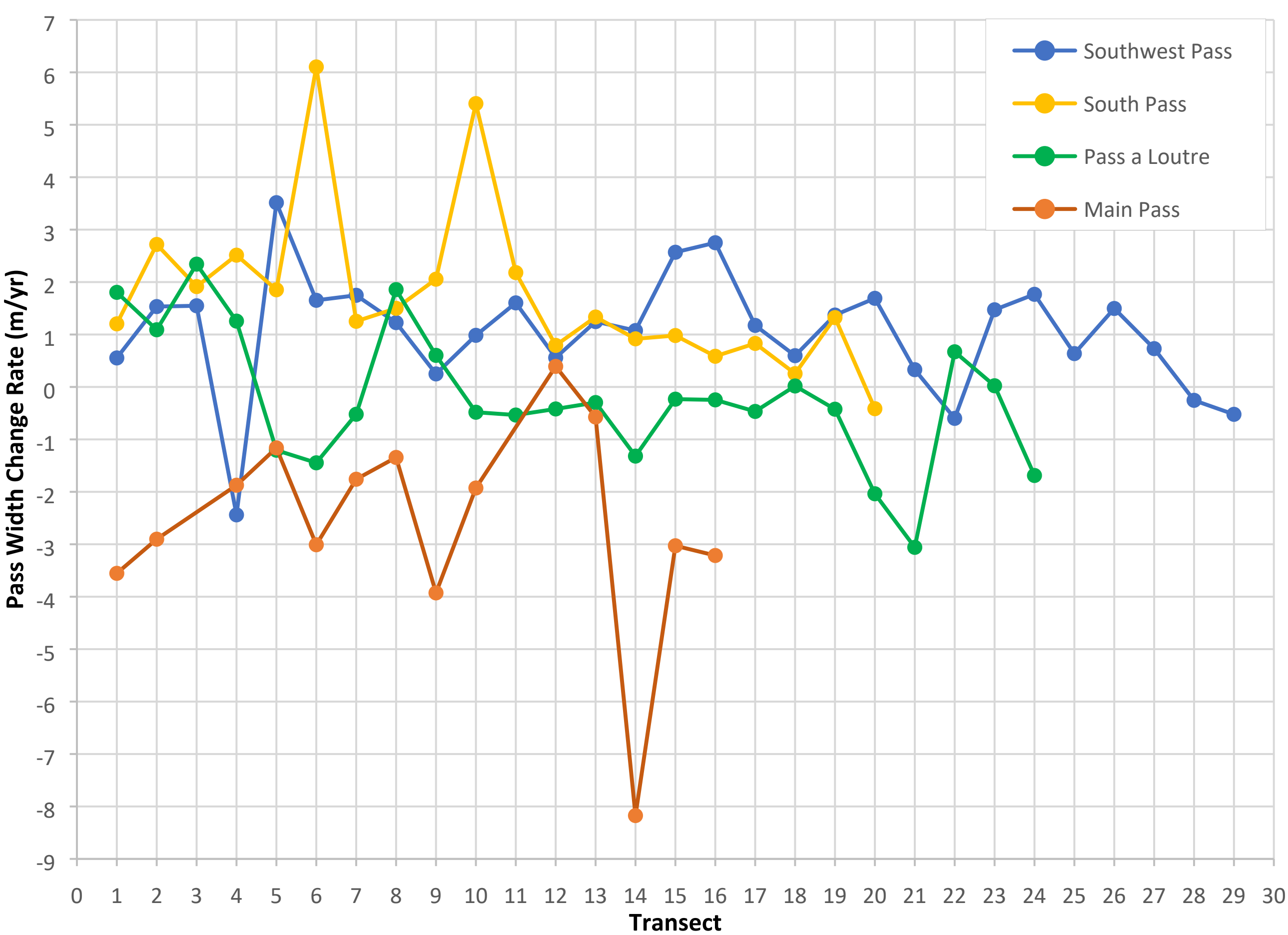

Fig. 10. Pass width change rate, from 1949 to 2019, by transect and area of interest.

Table 3
Comparison of the change rates in AOI channel widths between the historical period (1949 to 2013) and the dieback/recovery period (2013 to 2019).

Reach	Change in Pass Width (m/yr)	
	1949–2013	2013–2019
Main Pass	−3.20	−1.70
Pass a Loutre	−0.12	3.34
South Pass	2.49	1.95
Southwest Pass	0.84	5.72

at specific transects. For example, the width of Main Pass MP14, decreased at a rate of 8 m/yr due to the vegetative establishment of a shallow river area near the left bank of the Pass. Southwest Pass had the largest variation in change rates between periods with widening by 0.84 m/yr from 1949 to 2013, but increasing substantially to 5.72 m/yr between 2013 and 2019. The differences in change rates during the historical period are partially due to dredging and armoring of some channel reaches, vegetation type along channel banks, and impacts from previous disturbance events, while differences in change rates during the dieback/recovery periods are largely due to changes to *Phragmites* along the banks of the AOI channels.

4. Conclusions

The objectives of this study were to use satellite imagery to evaluate spatial and temporal changes in the Mississippi River Delta before, during, and after a *Phragmites* dieback event. Vegetation cover and the FQI were used to assess spatial and temporal changes in wetland condition, resilience, and recovery (Suir and Sasser, 2017). These species level assessments showed the MRD was a *Phragmites*-dominated landscape with high coverage values prior to the hurricane period. The landscape experienced decreasing coverage and FQI values during the hurricane period, and low and nominally increasing vegetation cover and quality through the dieback and recovery periods. These trends are typical in disturbed and distressed systems where vigorous and dominant wetland plants are encroached upon or replaced by lower quality invasive or disturbance species. These findings were corroborated with multi-temporal NDVI analyses, which showed an active delta landscape with below typical plant biomass/health in the hurricane and dieback periods, but recovered to NDVI values that are more typical for the MRD during the recovery period. These findings were also corroborated and extended using spatial and temporal hot spot analyses, which showed *Phragmites* dieback locations and areas of recovery.

Class-level assessments were used to evaluate dieback impacts on *Phragmites* patch dynamics (i.e., area, shape, edge, and adjacency) which provide useful measures of how *Phragmites* stands changed spatially over time. Although some AOIs experienced atypical trends in landscape metric values, most trends were indicative of wetland areas that experienced event-related stress during the hurricane and dieback periods, but then experienced some level of rebound during the recovery period. The channel morphology assessment provides a longer range of data to assess historical trends in relation to changes during the recent hurricane, dieback, and recovery periods. While all channels experienced shortening since the 1940s, changes in channel width were dissimilar for some AOIs. The class-level metrics can be used in addition to the measures of channel morphology to assess impacts on navigable waters, as well as the extent and location of areas most susceptible to erosion or plant species replacement.

Aquatic plants can protect Federal navigation channels and ports from wave action and other erosive energies. In addition to monitoring the distribution of foundational plants, quantifying the health, decline, and conversion of aquatic plants, remote assessments of wetland landscapes can provide operational value to stakeholders by assessing the impact of those changes on navigation (dredging), flood risk reduction, and ecosystem health. Furthermore, the identification of hot spot areas can assist in the planning and implementation of future restoration and management activities. The results of this study show the combination of remotely collected and in situ data can provide enhanced spatial and temporal measures of wetland plant extent and condition as a function of landscape level dynamics. Moreover, these data can assist in advancing environmental studies by providing a basis to target future data collections and analysis efforts, resulting in time and budget savings in the planning and study process. This study serves as a methodological basis for deriving vegetation trend assessments and integrating those results with landscape metrics to prioritize areas of interest; all of which are essential for effective management and mitigation of aquatic nuisance vegetation.

Funding

Funding for this research and paper was provided by the US Army Corps of Engineers Aquatic Plant Control Research Program.

CRediT authorship contribution statement

Glenn M. Suir: Conceptualization, Funding acquisition, Methodology, Data curation, Writing – original draft. **Christina L. Saltus:** Data curation, Writing – review & editing. **Molly K. Reif:** Funding acquisition, Writing – review & editing.

Declaration of Competing Interest

The authors declare that they have no known competing financial interests or personal relationships that could have appeared to influence the work reported in this paper.

Acknowledgment

This study was funded by the U.S. Army Corps of Engineers Aquatic Plant Control Research Program. The authors are grateful to Dr. Rodrigo Diaz and Dr. Ian Knight for their guidance and the ground verification data.

References

Alber, M., Swenson, E.M., Adamowicz, S.C., Mendelssohn, I.A., 2008. Salt marsh dieback: an overview of recent events in the US. Estuar. Coast. Shelf Sci. 80 (1), 1–11.
American Association of Port Authorities. 2018. 2018 U.S. Port Rankings by Cargo Tonnage. https://www.aapa-ports.org/unifying/content.aspx?ItemNumber=21048.
An, N., Price, K.P., Blair, J.M., 2013. Estimating above-ground net primary productivity of the tallgrass prairie ecosystem of the central great plains using AVHRR NDVI. Int. J. Remote Sens. 34 (11), 3717–3735.
Batker, D., De La Torre, I., Costanza, R., Swedeen, P., Day, J., Boumans, R., Bagstad, K., 2010. Gaining ground: wetlands, hurricanes, and the economy: the value of restoring the Mississippi River Delta. Envtl. L. Rep. News & Analysis 40, 11106.
Bourdaghs, M., Johnston, C.A., Regal, R.R., 2006. Properties and performance of the floristic quality index in Great Lakes coastal wetlands. Wetlands 26 (3), 718–735.
Broussard III, W.P., G.M. Suir, and J.M. Visser. 2018. UAS and satellite imagery collections in a coastal intermediate marsh to determine the land-water interface, vegetation types, and NDVI values. ERDC/TN WRAP-18-1. U.S. Army Engineer Research and Development Center, Vicksburg, Mississippi.
Carle, M.V., 2013. Spatial Structure and Dynamics of the Plant Communities in a Pro-Grading River Delta: Wax Lake Delta, Atchafalaya Bay, Louisiana. Louisiana State University, Baton Rouge, LA, USA. PhD Dissertation.
Carle, M.V., Sasser, C.E., Roberts, H.H., 2015. Accretion and vegetation community change in the Wax Lake Delta following the historic 2011 Mississippi River flood. J. Coastal Res. 313, 569–587.
Chaiwongsaen, N., Choowong, M., 2019. Assessment of the Lower Ping River's riverbank erosion and accretion, Northern Thailand using geospatial technique; implication for river flow and sediment load management.
Chander, G., Markham, B.L., Helder, D.L., 2009. Summary of current radiometric calibration coefficients for Landsat MSS, TM, ETM+, and EO-1 ALI sensors. Remote Sens. Environ. 113 (5), 893–903.
Choudhary, J., Ohri, A., Kumar, B., 2015. December. Spatial and statistical analysis of road accidents hot spots using GIS. 3rd Conference of Transportation Research Group of India (3rd CTRG).
Coastal Protection and Restoration Authority (CPRA) of Louisiana. 2019. Coastwide Reference Monitoring System-Wetlands Monitoring Data. Retrieved from Coastal

Information Management System (CIMS) database. http://cims.coastal.louisiana.gov. Accessed 27 July 2019.
Coleman, J.M., Roberts, H.H., Stone, G.W., 1998. Mississippi River Delta: an overview. J. Coastal Res. 14 (3), 699–716.
Couvillion, B.R., Barras, J.A., Steyer, G.D., Sleavin, W., Fischer, M., Beck, H., Trahan, N., Griffin, B., Heckman, D., 2011. Land Area Change in Coastal Louisiana from 1932 to 2010: Scientific Investigations Map 3164. U.S. Geological Survey, Reston, VA.
Couvillion, B.R., Fischer, M.R., Beck, H.J., Sleavin, W.J., 2016. Spatial configuration trends in coastal Louisiana from 1985 to 2010. Wetlands 36 (2), 347–359.
Cretini, K.F., Visser, J.M., Krauss, K.W., Steyer, G.D., 2011. CRMS vegetation analytical team framework—Methods for collection, development, and use of vegetation response variables: U.S. Geological Survey Open-File Report 2011–1097.
Cretini, K.F., Visser, J.M., Krauss, K.W., Steyer, G.D., 2012. Development and use of a floristic quality index for coastal Louisiana marshes. Environ. Monit. Assess. 184 (4), 2389–2403.
Cronin, J.T., Johnston, J., Diaz, R., 2020. Multiple potential stressors and dieback of *Phragmites australis* in the Mississippi River Delta. Wetlands 40 (6), 2247–2261.
Datt, B., 1999. A new reflectance index for remote sensing of chlorophyll content in higher plants: tests using Eucalyptus leaves. J. Plant Physiol. 154 (1), 30–36.
Day, J.W., Britsch, L.D., Hawes, S.R., Shaffer, G.P., Reed, D.J., Cahoon, D., 2000. Pattern and process of land loss in the Mississippi Delta: a spatial and temporal analysis of wetland habitat change. Estuaries Coasts 23 (4), 425. https://doi.org/10.2307/1353136.
De Jager, N.R., Fox, T.J., 2013. Curve fit: a pixel-level raster regression tool for mapping spatial patterns. Methods Ecol. Evol. 4 (8), 789–792.
Duke, N.C., Bell, A.M., Pederson, D.K., Roelfsema, C.M., Nash, S.B., 2005. Herbicides implicated as the cause of severe mangrove dieback in the Mackay region, NE Australia: consequences for marine plant habitats of the GBR World Heritage Area. Mar. Pollut. Bull. 51 (1–4), 308–324.
Environmental Systems Research Institute (ESRI). 2012. ArcGIS Desktop Release 10.7.1. Redlands, CA.
Environmental Systems Research Institute (ESRI). 2020. ArcGIS Pro Release 2.5.2. Redlands, CA.
Folse, T.M., L.A. Sharp, J. West, M.K. Hymel, T.E. McGinnis, D. Weifenbach, W.M. Boshart, L.B. Rodrigue, D.C. Richardi, W.B. Wood, and C.M. Miller. 2014. A standard operating procedures manual for the coast-wide reference monitoring system-wetlands: methods for site establishment, data collection, and quality assurance/quality control. Louisiana coastal protection and restoration authority, Office of Coastal Protection and Restoration. Baton Rouge, LA. 228 pp.
Gianopulos, K. 2014. Coefficient of conservatism database development for wetland plants occurring in the Southeast United States. North Carolina Dept. of Environment & Natural Resources, division of water resources: wetlands branch. Report to the EPA, region 4.
Hauber, D.P., Saltonstall, K., White, D.A., Hood, C.S., 2011. Genetic variation in the common reed, *Phragmites australis*, in the Mississippi River Delta Marshes: evidence for multiple introductions. Estuaries Coasts 34 (4), 851–862.
He, H.S., DeZonia, B.E., Mladenoff, D.J., 2000. An aggregation index (AI) to quantify spatial patterns of landscapes. Landscape Ecol. 15 (7), 591–601.
Howard, R.J., Turluck, T.D., 2013. *Phragmites australis* expansion in a restored brackish marsh: documentation at different time scales. Wetlands 33 (2), 207–215.
ITT Visual Information Solutions Inc. 2009. ENVI Atmospheric Correction Module: QUAC and FLAASH User's Guide v. 4.7. ITT Visual Information Solutions Inc.: Boulder, CO.
Jensen, J.R., 2015. Introductory Digital Image Processing: A Remote Sensing Perspective. Prentice Hall Press.
Jollineau, M.Y., Howarth, P.J., 2008. Mapping an inland wetland complex using hyperspectral imagery. Int. J. Remote Sens. 29 (12), 3609–3631. https://doi.org/10.1080/01431160701469099.
Kalnay, E., Kanamitsu, M., Kistler, R., Collins, W., Deaven, D., Gandin, L., Iredell, M., Saha, S., White, G., Woollen, J., Zhu, Y., Leetmaa, A., Reynolds, R., Chelliah, M., Ebisuzaki, W., Higgins, W., Janowiak, J., Mo, K.C., Ropelewski, C., Wang, J., Jenne, R., Joseph, D., 1996. The NCEP/NCAR 40-year reanalysis project. Bull. Am. Meteorol. Soc. 77 (3), 437–471.
Karr, J.R., Chu, E.W., 1997. Biological monitoring and assessment: using multimetric indexes effectively. EPA/235/R97/001. University of Washington, Seattle, WA.
Kaufmann, P.R., 2000. Physical Habitat Characterization: Non-wadeable Rivers. Environmental Monitoring and Assessment Program–Surface Waters: Field Operations and Methods for Measuring the Ecological Condition of Non-Wadeable Rivers and Streams, EPA/620/R-00/007, US EPA, Cincinnati, Ohio, pp. 6–1.
Knight, I.A., J.T. Cronin, M. Gill, J.A. Nyman, B.E. Wilson, and R. Diaz. 2020. Investigating plant phenotype, salinity, and infestation by the roseau cane scale as factors in the die-back of *Phragmites australis* in the Mississippi River Delta, USA. Wetlands, pp. 1–11.
Kupfer, J.A., 2012. Landscape ecology and biogeography: rethinking landscape metrics in a post-FRAGSTATS landscape. Prog. Phys. Geogr. 36 (3), 400–420.
Lindstedt, D.M., Swenson, E.M., Reed, D., Twilley, R., Mendelssohn, I.A., 2006. The Case of the Dying Marsh Grass. Report submitted to the Louisiana Department of Natural Resources, Baton Rouge, LA.
Little, A., 2013. Sampling and analyzing wetland vegetation. In: Anderson, J.T., Davis, C. A. (Eds.), Wetland Techniques. Springer Netherlands, Dordrecht, pp. 273–324. https://doi.org/10.1007/978-94-007-6860-4_5.
McConnell, H.S., 1954. A Classification of the Coccid Family *Aclerdidae* (Coccoidea, Homoptera). Bull. Maryland Agric. Exp. Stat. A75, 1–121.
McGarigal, K. 2015. FRAGSTATS help. Pieejams: http://www.umass.edu/landeco/research/fragstats/documents/fragstats.help, v4.
McGarigal, K., Cushman, S.A., Ene, E., 2012. FRAGSTATS v4: Spatial Pattern Analysis Program for Categorical and Continuous Maps. The University of Massachusetts, Amherst.
Mutanga, O., Adam, E., Cho, M.A., 2012. High density biomass estimation for wetland vegetation using WorldView-2 imagery and random forest regression algorithm. Int. J. Appl. Earth Obs. Geoinf. 18, 399–406.
Osland, M.J., Day, R.H., Michot, T.C., Lambrinos, J., 2020. Frequency of extreme freeze events controls the distribution and structure of black mangroves (*Avicennia germinans*) near their northern range limit in coastal Louisiana. Divers. Distrib. 26 (10), 1366–1382. https://doi.org/10.1111/ddi.13119.
Plitsch, E., 2017. 2016 Operations, Maintenance, and Monitoring Report for West Bay Sediment Diversion (MR-03). Coastal Protection and Restoration Authority of Louisiana, New Orleans, LA.
Reif, M.K., Macon, C.L., Wozencraft, J.M., 2011. Post-Katrina land-cover, elevation, and volume change Assessment along the south shore of Lake Pontchartrain, Louisiana, U.S.A. J. Coastal Res. 30–39, 10062.
Sarkar, A., 2004. River Bank Erosion: Geomorphology and Environment. In Geomorphology and Environment. In: Singh, S., Sharma, H.S., De, S.K., Publications, A.C.B., Kolkata, I. (Eds.), River Bank Erosion: Geomorphology and Environment. In Geomorphology and Environment.
Schmidt, G.L., C.B. Jenkerson, J. Masek, E. Vermote, and F. Gao. 2013. Landsat ecosystem disturbance adaptive processing system (LEDAPS) algorithm description: U.S. Geological Survey Open-File Report 2013–1057, 17 p.
Sims, D.A., Gamon, J.A., 2002. Relationships between leaf pigment content and spectral reflectance across a wide range of species, leaf structures and developmental stages. Remote Sens. Environ. 81 (2-3), 337–354.
Steyer, G.D., Couvillion, B.R., Barras, J.A., 2013. Monitoring vegetation response to episodic disturbance events by using multitemporal vegetation indices. J. Coastal Res. 63 (sp1), 118–130.
Suir, G.M., Evers, D.E., Steyer, G.D., Sasser, C.E., 2013. Development of a reproducible method for determining quantity of water and its configuration in a marsh landscape. J. Coastal Res. 63 (sp1), 110–117.
Suir, G M., W.R., Jones, A.L. Garber, and J.A. Barras., 2014. Pictorial Account and Landscape Evolution of the Crevasses near Fort St. Philip, Louisiana (No. 2). U.S. Army Corps of Engineers. https://pubs.er.usgs.gov/publication/70094484.
Suir, G.M., Saltus, C.L., Johnston, J.B., Barras, J.A., 2011. Development of methodology to classify historical panchromatic aerial photography. Analysis of landscape features on point au Fer Island, Louisiana from 1956 to 2009: a case study. No. ERDC/EL-TR-11-17. Engineer Research and Development Center, environmental laboratory, Vicksburg, Mississippi.
Suir, G.M., Saltus, C.L., Reif, M.K., 2018. Geospatial assessments of *Phragmites australis* die-off in south Louisiana: preliminary findings. U.S. Army Engineer Research and Development Center. ERDC/EL TR18-9, Vicksburg, Mississippi.
Suir, G.M., Saltus, C.L., Sasser, C.E., Harris, J.M., 2021. Evaluating Drone Truthing as an Alternative to Ground Truthing: An Example with Wetland Plant Identification. APCRP Technical Notes Collection. In: ERDC/TN, APCRP-MI-9.. US Army Engineer Research and Development Center, Vicksburg, MS.
Suir, G.M., Sasser, C.E., 2017. Floristic Quality Index of Restored Wetlands in Coastal Louisiana (no. ERDC/EL TR-17-15). Engineer Research and Development Center, Environmental Lab Vicksburg, Mississippi.
Suir, G.M., Sasser, C.E., 2019. Use of NDVI and landscape metrics to assess effects of riverine inputs on wetland productivity and stability. Wetlands 39 (4), 815–830.
Suir, G.M., Sasser, C.E., Harris, J.M., 2020. Use of remote sensing and field data to quantify the performance and resilience of restored Louisiana Wetlands. Wetlands 40 (6), 2643–2658.
White, D.A., 1993. Vascular plant community development on mudflats in the Mississippi River delta, Louisiana, USA. Aquat. Bot. 45 (2–3), 171–194.